



Brain encoding of acupuncture sensation — Coupling on-line rating with fMRI

Citation

Napadow, Vitaly, Rupali P. Dhond, Jieun Kim, Lauren LaCount, Mark Vangel, Richard E Harris, Norman Kettner, and Kyungmo Park. 2009. "Brain Encoding of Acupuncture Sensation — Coupling on-Line Rating with fMRI." *NeuroImage* 47 (3) (September): 1055–1065. doi:10.1016/j.neuroimage.2009.05.079.

Published Version

doi:10.1016/j.neuroimage.2009.05.079

Permanent link

<http://nrs.harvard.edu/urn-3:HUL.InstRepos:36638454>

Terms of Use

This article was downloaded from Harvard University's DASH repository, and is made available under the terms and conditions applicable to Other Posted Material, as set forth at <http://nrs.harvard.edu/urn-3:HUL.InstRepos:dash.current.terms-of-use#LAA>

Share Your Story

The Harvard community has made this article openly available.
Please share how this access benefits you. [Submit a story](#).

[Accessibility](#)

Published in final edited form as:

Neuroimage. 2009 September ; 47(3): 1055–1065. doi:10.1016/j.neuroimage.2009.05.079.

Brain encoding of acupuncture sensation - coupling on-line rating with fMRI

Vitaly Napadow^{1,2,*}, Rupali P. Dhond^{1,2}, Jieun Kim^{1,3}, Lauren LaCount¹, Mark Vangel^{1,4}, Richard E Harris⁵, Norman Kettner², and Kyungmo Park^{1,3,*}

¹ MGH/HMS/MIT Martinos Center for Biomedical Imaging, Massachusetts General Hospital, Boston, MA

² Department of Radiology, Logan College of Chiropractic, Chesterfield, MO

³ Department of Biomedical Engineering, Kyunghee University, Yongin, Korea

⁴ MGH GCRC Biomedical Imaging Core, Charlestown, MA

⁵ Chronic Pain and Fatigue Research Center, Department of Anesthesiology, University of Michigan, Ann Arbor, MI

Abstract

Acupuncture-induced sensations have historically been associated with clinical efficacy. These sensations are atypical, arising from sub-dermal receptors, and their neural encoding is not well known. In this fMRI study, subjects were stimulated at acupoint PC-6, while rating sensation with a custom-built, MR-compatible potentiometer. Separate runs included real (ACUP) and sham (SHAM) acupuncture, the latter characterized by non-insertive, cutaneous stimulation. FMRI data analysis was guided by the on-line rating timeseries, thereby localizing brain correlates of acupuncture sensation. Sensation ratings correlated with stimulation more ($p < 0.001$) for SHAM ($r = 0.63$) than for ACUP ($r = 0.32$). ACUP induced stronger and more varied sensations with significant persistence into no-stimulation blocks, leading to more runtime spent rating low and moderate sensations compared to SHAM. ACUP sensation correlated with activation in regions associated with sensorimotor (SII, insula) and cognitive (dorsomedial prefrontal cortex (dmPFC)) processing, and deactivation in default-mode network (DMN) regions (posterior cingulate, precuneus). Compared to SHAM, ACUP yielded greater activity in both anterior and posterior dmPFC and dlPFC. In contrast, SHAM produced greater activation in sensorimotor (SI, SII, insula) and greater deactivation in DMN regions. Thus, brain encoding of ACUP sensation (more persistent and varied, leading to increased cognitive load) demonstrated greater activity in both cognitive/evaluative (posterior dmPFC) and emotional/interoceptive (anterior dmPFC) cortical regions. Increased cognitive load and dmPFC activity may be a salient component of acupuncture analgesia - sensations focus attention and accentuate bodily awareness, contributing to enhanced top-down modulation of any nociceptive afference and central pain networks. Hence, acupuncture may function as a somatosensory-guided mind-body therapy.

© 2009 Elsevier Inc. All rights reserved

*Corresponding Addresses: Vitaly Napadow, PhD Martinos Center for Biomedical Imaging 149 Thirteenth St. #2301 Charlestown, MA 02129, Kyungmo Park, PhD Department of Biomedical Engineering, room 705 Kyunghee University Yongin, Gyeonggi, Korea, 466-701.

Publisher's Disclaimer: This is a PDF file of an unedited manuscript that has been accepted for publication. As a service to our customers we are providing this early version of the manuscript. The manuscript will undergo copyediting, typesetting, and review of the resulting proof before it is published in its final citable form. Please note that during the production process errors may be discovered which could affect the content, and all legal disclaimers that apply to the journal pertain.

INTRODUCTION

Acupuncture therapy originated in China over 2500 years ago, but its mechanisms of action are not well understood. Acupuncture involves puncture of the skin with a thin, solid shaft needle. Subsequent manipulation of this needle can then be accomplished by twisting the needle handle between two fingers. The associated subdermal trauma serves to stimulate nerve receptors both directly and indirectly through mechanical coupling via the connective tissue surrounding the needle (Langevin et al., 2002). The sensations induced by acupuncture needling are one of its unique characteristics. These sensations, sometimes referred to as *deqi* (Kong et al., 2007a; Park et al., 2002; Vincent et al., 1989), include aching, numbness, tingling, and even warmth, encompassing several different psychophysical categories, including both pain and non-pain qualities. Importantly, the attainment of these sensations in a clinical setting has been linked in many traditional Chinese medicine texts (Cheng, 1996) with successful therapeutic outcomes. *Deqi* sensation produces greater local blood flow at the needle site compared to simple needle insertion (Sandberg et al., 2003). Furthermore, experimental studies have found correlation between the intensity of different acupuncture sensations and subsequent analgesia (Kong et al., 2005). The brain correlates of acupuncture sensation might suggest how and why this sensation is connected to therapeutic outcome - a connection that is currently unknown.

The varied sensations evoked by acupuncture may arise following distinct combinations of afferent signaling. For instance, Wang et al. used electrophysiology to associate different sensations (“numbness,” “distention,” and “soreness”) to different fiber types (II, III, and IV respectively) (Wang et al., 1985). Moreover, as acupuncture sensations arise from deeper receptors located in fascia and/or muscle tissue, they are likely to have different somatosensory qualities and thus a relatively greater “novelty” compared to the more pedestrian sensations elicited by tactile stimulation of cutaneous receptors. While brain response to acupuncture likely plays an important role in therapeutic outcome, the specific neural correlates of acupuncture sensation have not been evaluated in an explicit manner.

Neuroimaging of acupuncture stimulation using functional MRI (fMRI) has been typically performed using a block design. The needle, inserted prior to the scan, is stimulated continuously for a duration ranging from 30 seconds to 2 minutes during several ON blocks, interspersed between several OFF, or no-stimulation rest blocks. When using this block design as a general linear model (GLM) regressor to the fMRI data, an underlying assumption is that mechanoreceptor and nociceptor-associated afference, as well as the conscious perception and evaluation of this afference, is coincident with needle stimulation. However, recent studies have begun to question the equivalence of stimulation with sensation in block-design acupuncture experiments (Ho et al., 2008). As fMRI response to acupuncture has been found to necessitate conscious (awake) perception of the stimulation (Wang et al., 2007), the neural correlates of acupuncture sensation are likely to be important to brain processing during acupuncture.

Exploring the neural correlates of sensation has been previously accomplished with percept-related fMRI - a technique wherein the subject performs on-line rating of sensation with the aid of visual guidance. The rating timeseries is then used to form GLM regressor(s) to the concurrently collected fMRI data. This approach has been used successfully to find the neural correlates of prickle sensation (Davis et al., 2002), as well as the brain regions encoding both thermal and spontaneous pain in chronic pain patients (Baliki et al., 2006).

In our study, we have employed percept-related fMRI to evaluate the neural correlates of acupuncture sensation. We hypothesized that acupuncture sensation would persist into OFF-blocks following the stimulation ON-block, and that this persistence would be more robust for

real (both cutaneous and deep receptors), compared to sham (cutaneous only) acupuncture. We further hypothesized that inherently atypical acupuncture sensations would evoke different rating-associated brain response compared to that associated with sham acupuncture, which is characterized by more conventional cutaneous-derived afferent input.

METHODS

Subjects and Experimental Design

Fifteen (15) healthy, right handed (Oldfield, 1971) adults (8 female, 21-33 years of age) received both real manual acupuncture (ACUP) and sham acupuncture (SHAM) in one experimental session. Subjects were recruited via fliers/newsletters adhering to MGH guidelines for distribution at neighboring academic institutions and hospitals. Subjects were screened to assure their safety and compatibility with MRI recording. All participants in the study provided written informed consent in accordance with the Human Research Committee of the Massachusetts General Hospital.

Both ACUP and SHAM runs consisted of a block design with five 30-second stimulation blocks (ON), interspersed between six 30-second rest blocks (OFF). The total time for the block-design run was 5.5 minutes (Figure 1). The order of ACUP and SHAM was pseudo-randomized across subjects to mitigate order effects. These two runs were also separated by structural and rest fMRI scans which ensured at least 25 minutes between successive stimulations. While adequate washout for acupuncture is unknown, sensation ratings taken before needle insertion (real or sham) in the latter stimulation scan confirmed that subjects experienced no lasting sensations from the former stimulation scan. On-line acupuncture sensation was rated throughout both runs (see below).

All acupuncture was performed by the same licensed (and experienced) acupuncturist at acupoint PC-6 on the left forearm. This acupoint, which is on the volar aspect of the forearm, is 2 cun (approximately 5cm) proximal to the transverse wrist crease, between the tendons of the palmaris longus and flexor carpi radialis muscles. This point has been used clinically for cardiac conditions, as well as to control nausea and vomiting. It was chosen for this study due to its location overlying the median nerve and noted sensitivity, thus making it a good candidate to study interesting acupuncture-induced sensation patterns. For ACUP, acupuncture was performed by first inserting a non-magnetic (pure silver), 0.23mm diameter, 30mm long acupuncture needle (Asahi Industry, Inc., Kawaguchi, Japan) into PC-6 to a depth of approximately 1.5cm. During stimulation, the needle was manually twirled ($\sim\pm 180^\circ$) approximately at 0.5 Hz.

For SHAM, needle insertion was first simulated by briskly poking the skin over PC-6 with a 5.88 von Frey monofilament passed through a needle guide tube (similar to the one used for ACUP). During the scan run, the acupuncturist performed non-invasive cutaneous stimulation over the acupoint (tapping at 0.5 Hz) using the same monofilament. Subjects were acupuncture-naïve and were informed that there would be “different forms” of acupuncture during fMRI. Subjects lay supine in the scanner with their vision of distal body regions blocked by the MRI head coil, preventing them from viewing the intervention occurring at their periphery. SHAM aimed to control for both tactile stimulation of cutaneous somatosensory receptors over the acupoint, as well as the cognitive processing induced by subjects expecting “acupuncture” stimulation. Hence, the “specific effect” in ACUP that is not controlled for by SHAM is the stimulation of deep (subdermal) somatosensory receptors by the “invasive” acupuncture needle. Furthermore, non-insertive sham acupuncture stimulation is typically used as a placebo control in many acupuncture clinical trials; thus using this control in our study is warranted and relevant to the field.

Psychophysical Sensation Data Collection and Analysis

During each scan run (on-line) as well as after (retrospective), subjects were asked to rate the sensation induced by ACUP and SHAM stimulation. For on-line rating, subjects were not informed about the block-design paradigm in the experiment, and were instructed to rate the sensation continuously throughout the entire run. On-line rating was accomplished by the use of a custom-built MR-compatible handheld potentiometer and rotating knob connected to a visual display projecting an intensity scale. While the potentiometer knob was set to traverse the entire rating range with minimal thumb/index finger twisting, sensitivity was limited by a finite fMRI-induced noise floor in the signal. The device was held in the dominant right arm, opposite to the acupuncture-stimulated arm. The visual feedback consisted of a 100 point visual analog scale (VAS), which contained only the following guidewords: “none” corresponding to 0, and “unbearable” corresponding to 100. Intermediate guidewords also included “mild,” which corresponded to a value of 20, “moderate,” which corresponded to 50, and “strong,” which corresponded to 80. Potentiometer response was acquired at 200 Hz with a laptop running Labview software (Labview 7.0, DAQCard 6024E, National Instruments, Austin, Texas).

For retrospective psychophysical data collection, following the ACUP and SHAM portions of the scan session, subjects were presented with a 10-point VAS and were asked to rate the intensity of different sensations they felt during the active stimulation run. The rated sensations were commonly associated with the experience of *deqi* (i.e. aching, soreness, pressure, heaviness, fullness, warmth, cool, numbness, tingling, and dull pain).

Several analyses of the on-line ratings were performed. Spearman correlation coefficients were calculated to investigate the relationship between the on-line sensation ratings and the block design (which matches needle stimulation). A spectral analysis of the ratings time series was performed (MATLAB, Mathworks Inc., Natick, MA) to compare the power spectral density (PSD) between ACUP and SHAM. Timeseries were first linearly detrended to remove any DC offset. We then calculated power within the stimulation frequency band ($0.0166 \pm 0.003\text{Hz}$), corresponding to our stimulus block design (30seconds OFF and 30seconds ON), as well as a low frequency band ($0.001\text{-}0.0136\text{Hz}$) below the stimulation band. The PSD of both frequency bands was normalized by dividing by the total power (up to the first harmonic of the stimulation frequency, or 0.03Hz). We also calculated the time that subjects spent rating minimal (0-10), low (10-40), moderate (40-70), and high (70-100) intensity sensations. Comparisons between ACUP and SHAM were performed using a paired Students' t-test, significant at $\alpha < 0.05$. The rating time series were also used as regressors in the fMRI GLM analysis (described below).

We performed both a prevalence and intensity analysis for retrospective sensations. A sensation was counted as present if the intensity was greater than 0.5. Subjects were also asked to assess the intensity of throbbing, sharp pain (this sensation is not considered to be characteristic of *deqi*), and anxiety/relaxation. The anxiety/relaxation scale ranged from very anxious (5) to fully relaxed (-5), with a zero (0) value signifying neither anxious nor relaxed. Additionally, subjects were asked to assess the extent of “spreading” that may have occurred for any of the listed sensations. A modified version of this procedure has been successfully used by our group in the past to assess psychophysical response in conjunction with neuroimaging (Hui et al., 2005; Napadow et al., 2005). In order to quantify the total intensity of *de qi* experienced we used the MGH Acupuncture Sensation Scale Index (*MASS-Index* (Kong et al., 2007a)). This index attempts to balance breadth and depth of sensations as well as the number of different sensations chosen by the subject. The MASS index and individual sensation intensities were compared between stimulation groups using a paired t-test, significant at $p < 0.05$ (SPSS 10.0.7, Chicago, Illinois). Furthermore, frequency counts of specific sensations were compared between stimulation type with a Pearson Chi-squared test, significant at $p < 0.05$. An omnibus

test (Fisher's combined probability test) was used to test if the commonality of sensations elicited by ACUP differed from that elicited by SHAM. These data were also used in a previous report correlating acupuncture sensation with acupuncture effects on resting state connectivity (Dhond et al., 2008).

Imaging data collection and analysis

FMRI Data were acquired using a 3T Siemens Tim Trio MRI System (Siemens Medical, Erlangen, Germany) equipped for echo planar imaging with a 12-channel head coil. During scanning, subjects remained in the supine position with their heads immobilized by cushioned supports. Subjects wore earplugs throughout the experiment to attenuate MRI gradient noise. Structural scans consisted of a T1-weighted anatomical (TR/TE = 2.73/3.19 ms, flip angle = 7°, FOV = 256 × 256 mm; slice thickness = 1.33 mm) and a multi-echo fieldmap scan (f.a. = 55°, TR/TE1/TE2 = 500/3.38/5.84 ms). Blood oxygenation level-dependent (BOLD) functional imaging was performed using a gradient echo T2*-weighted pulse sequence (TR/TE = 3000/30 ms, flip angle = 90°, FOV = 200 × 200 mm, 48 coronal slices, slice thickness = 3.0 mm with 0.6 mm interslice gap, matrix = 64 × 64, 110 time points for a total of 5.5 min). Image collection was preceded by 5 dummy scans. Coronal slices were used to minimize susceptibility artifact (gradient distortion) in subcortical limbic regions (Ojemann et al., 1997).

Data analysis was performed using a combination of analysis packages including FSL (FMRIB's Software Library) and AFNI. Functional data were pre-processed to correct for magnetic field inhomogeneities caused by magnetic susceptibility differences in neighboring tissues within the head (FSLFUGUE) and motion corrected to compensate for any head movements using a linear (affine) transformation procedure (FSL-FLIRT). Brain extraction was performed on functional data using FSL-BET while skull stripping of structural data for alignment utilized Freesurfer software. Functional data were smoothed using a Gaussian kernel of FWHM 5 mm; and high-pass temporal filtering ($f = 1/330$ Hz) was also performed.

Single-Subject fMRI and Structural Data Analysis

Statistical parametric mapping at the single subject level was completed via a generalized linear model (GLM) by using FMRI Expert Analysis Tool (FEAT, FSL). The explanatory variable utilized in the general linear model (GLM) analysis was defined by the on-line sensation rating time series convolved with a canonical gamma function (SD= 3s, mean lag=6s). The on-line rating sensation was re-scaled to fall within the range of 0 to 1 (from the initial rating of 0 to 100). For comparison, we performed a separate, more traditional GLM analysis using the block design as explanatory variable. As our difference map results (see below) did not contain significant subcortical response, the resulting parameter estimates associated with both analyses were used in both a volumetric and surface-based group analysis, which provides better fidelity for cortical response.

In order to perform a surface-based group analysis, structural T1-weighted MPRAGE images from each subject were processed by the Freesurfer software package, which was used to generate a model of the cortical surface through intensity normalization, skull-stripping, segmentation, and tessellation of the gray/white matter interface surface (Dale et al., 1999). This reconstructed cortical surface was inflated using spring force and metric-preserving terms. The tessellated surface was also projected onto a unit sphere (spherical space), using algorithms that minimize metric distortions, thereby parameterizing the surface into a spherical-based coordinate system (Fischl et al., 1999).

Group fMRI Data Analysis

Surface-based group analysis was completed using the Freesurfer software package. The cortical surface of each subject brain was normalized to an average brain template by maximizing alignment of the folding patterns in a spherical representation, a process that provides accurate group-averaged statistical analysis over surface elements from topologically homologous regions in the brains of different subjects. Parameter estimates and their variance from each subject were mapped to surface space with a 0.5 projection fraction (half the distance between gray/white boundary and pial surface). Group maps for both ACUP and SHAM were generated with a one-sample t-test under mixed effects estimation (weighted least squares). A Difference map contrasting ACUP and SHAM was also created under a mixed effects model using a paired t-test. As sensation intensity was found to be significantly greater for ACUP compared to SHAM (see Results), the mixed effects model controlled for the mean sensation intensity calculated across the entire time series, using a covariate of no-interest. This difference map helps control for brain activity associated with cutaneous stimulation, placebo effects, and with performing a motor/rating task, as this task was performed for both ACUP and SHAM, and would be subtracted off in the difference map. Resultant statistical parametric maps were corrected for multiple comparisons using a Monte Carlo simulation (10,000 iterations) combining node-wise and cluster-wise probability thresholding. Significant clusters were retained with cluster-wise probability threshold of 0.05.

The volumetric group analysis for subcortical regions was performed by transforming subject level parameter estimates and their variance into MNI space, and performing single-sample and paired t-tests using a mixed effects model (FLAME, FSL). The results were corrected for multiple comparisons using Gaussian Random Field theory. Significant clusters were retained with cluster-wise probability threshold of 0.05.

RESULTS

All 15 subjects were able to complete both stimulation runs, however one subject was excluded from further fMRI GLM analysis because their on-line rating for SHAM was near zero (2.8 ± 1.9 , $\mu \pm \sigma$, on a scale of 0-100).

Psychophysics results

Both on-line rating and retrospective psychophysical data were collected. While notable inter-subject variability existed, particularly for ACUP (Supplementary Figures 1, 2), on-line acupuncture sensation timeseries demonstrated different patterns between ACUP and SHAM stimulation runs (Figure 2). The SHAM (Spearman's $r=0.63$) rating time series correlated better with the stimulation block design ($p<0.001$) compared to ACUP ($r=0.32$, Figure 2-B). Furthermore, while SHAM showed greater power ($p<0.05$) within the stimulation frequency band, ACUP showed greater power ($p<0.05$) within the low frequency band (Figure 3). This result was partly due to increased sensation persistence into the no-stimulation rest block following the stimulation block for ACUP compared to SHAM (Figure 2-C). However, some subjects had more unusual patterns of sensation response - occasionally with even more sensation during no-stimulation blocks than during stimulation blocks (Figure 2-A, Supplementary Figures 1,2). As a result, subjects spent more of the ACUP scan run rating low (10-40, $p<0.005$) and moderate (40-70, $p<0.05$) sensations, than during SHAM (Figure 4). In contrast, during SHAM, subjects spent significantly more time ($p<0.001$) rating minimal or no sensation (0-10), compared to ACUP. There was no difference in the time spent rating strong sensations ($p>0.1$).

Retrospective sensation ratings using the MASS scale were also collected and revealed different qualities and intensity of sensation (Figure 5). The MASS Index, a measure of overall

sensation intensity, was greater for ACUP compared to SHAM stimulation (paired t-test, $p < 0.01$). Interestingly, our on-line data corroborated this result, as average on-line rating intensity was greater ($p < 0.05$) for ACUP (29.2 ± 11.3) than for SHAM (20.7 ± 14.0). Additionally, MASS Index was correlated with average on-line rating intensity (ACUP: $r = 0.79$, $p < 0.001$; SHAM: $r = 0.74$, $p < 0.005$). Specific MASS sensations were also different, in intensity (0-10 scale) and prevalence, between the two stimulation runs. ACUP demonstrated greater intensity than SHAM for the following sensations: soreness (ACUP: 2.7 ± 2.6 , $\mu \pm \sigma$; SHAM: 1.3 ± 1.8 ; $p < 0.05$), aching (ACUP: 3.8 ± 2.5 ; SHAM: 1.3 ± 1.8 ; $p < 0.005$), Fullness (ACUP: 1.5 ± 2.1 ; SHAM: 0.3 ± 0.5 ; $p < 0.05$), dull pain (ACUP: 4.2 ± 1.9 ; SHAM: 1.3 ± 1.8 ; $p < 0.001$), and spreading (ACUP: 2.2 ± 2.6 ; SHAM: 0.6 ± 1.0 ; $p < 0.05$). Interestingly, SHAM (-1.2 ± 2.4) was associated with greater ($p < 0.05$) relaxation compared to ACUP (0.2 ± 2.3). However, there was no significant difference in the intensity of sharp pain (ACUP: 3.5 ± 2.7 ; SHAM: 4.0 ± 3.1) or throbbing (ACUP: 2.4 ± 2.5 ; SHAM: 1.2 ± 2.1), sensations which have *not* been associated with deqi (Hui et al., 2007). In regard to sensation prevalence, an omnibus test (Fisher's combined probability test) found that ACUP and SHAM also differed in the types of sensations elicited ($p < 0.001$). The prevalence of "aching" (ACUP: 86.7% of subjects, SHAM: 40.0%, $p < 0.01$), "fullness" (ACUP: 46.7%, SHAM: 13.3%, $p < 0.05$), and "dull pain" (ACUP: 93.3%, SHAM: 40.0%, $p < 0.005$) was found to be greater for ACUP. It should also be noted that while sharp pain was reported for both ACUP and SHAM, when debriefed, most subjects who reported sharp pain described this sensation as only transient, occurring typically at the start of stimulation.

fMRI results

Group maps of the main effect for percept-related fMRI demonstrated many similarities between ACUP and SHAM (Figures 6,7, Tables 1,2). The sensation elicited by both stimulations was associated with activation in areas implicated in sensorimotor processing: bilateral SI, SII, posterior parietal (angular (angG) and supramarginal (SMG) gyri), anterior and posterior insula, supplementary motor area (SMA), and precentral gyrus (more left than right hemisphere). Sensation induced by both ACUP and SHAM was also associated with deactivation in the default-mode network (DMN) of brain regions, which constitutes regions known to more active during rest than during most externally focused tasks (Raichle et al., 2001). In our data, deactivation was found in the precuneus, posterior cingulate cortex (PCC), and inferior parietal lobule (IPL). Deactivation outside of the DMN was also found in medial occipital (visual) areas and right central sulcus (BA 3a). Higher cognitive areas, such as the dorsolateral prefrontal cortex (dlPFC, consistent with BA 9, 10, 44, 45, 46), were also modulated (mostly activated) bilaterally by both forms of stimulation. For ACUP, activation was also seen in the dorsomedial prefrontal cortex (dmPFC). For SHAM, activation was also seen in the caudate, putamen, cerebellum, and regions associated with sensorimotor processing, such as the posterior middle cingulate cortex (pmCC), and lateral occipital complex (LOC). Deactivation in default mode regions also included the ventromedial prefrontal cortex (vmPFC) and hippocampal formation.

A group difference map contrasting ACUP and SHAM was completed in order to better control for cutaneous tactile, placebo, and motor/rating task effects, as these aspects would play a role for both modes of stimulation. The ACUP-SHAM difference map noted several important differences between ACUP and SHAM (Figure 8, Table 3). Clusters with significant positive z-scores could arise from either greater ACUP activation, or greater SHAM deactivation. The inverse is true for clusters with significant negative z-scores. With this caveat in mind (and dissociated by group %-change for each cluster in Table 3), SHAM induced greater activation in sensorimotor processing regions including bilateral SI (BA 2), SII, and LOC. SHAM sensation was also correlated with greater activation in the left anterior insula. Furthermore, SHAM also induced greater deactivation in default-mode regions including PCC (both dorsal

and ventral), precuneus, vmPFC, IPL, and parahippocampus. Greater deactivation was also induced by SHAM in a medial parietal paracentral region, MTG/STG, and cuneus. However, ACUP induced greater activation in the dlPFC, and both the cognitive / evaluative (posterior) and emotional / interoceptive (anterior) subregions of the dmPFC, as anatomically and functionally parcellated by Amodio and Frith, as well as Steele and Lawrie (Amodio and Frith, 2006; Steele and Lawrie, 2004).

Comparing the above percept-related results to a more traditional analysis using the stimulation block design, some similar trends were noted in that SHAM induced greater activation in sensorimotor processing regions and deactivation in default-mode regions (Supplementary Figure 3). However, the block design group map for ACUP also demonstrated deactivation in the vmPFC and sub-genual anterior cingulate cortex (sgACC), while there was no activation in the dmPFC (which was activated in the percept-related analysis for ACUP). The block design group map for SHAM was very similar to the percept-related analysis, which was not surprising as SHAM ratings were significantly more similar to the block design than were ACUP ratings.

DISCUSSION

Our study applied percept-related fMRI to evaluate the neural correlates of an important component of acupuncture therapy - the sensation elicited by needle manipulation. We contrasted real ACUP with a non-insertive SHAM, and found that the sensations elicited by ACUP were qualitatively more complex, persisted after cessation of needle manipulation, and varied more appreciably between individuals. Furthermore, while substantial similarities existed in brain response to ACUP and SHAM, notably activation of the sensorimotor system and deactivation of the DMN, important differences were also found. Specifically, while SHAM sensation was associated with greater activation in sensorimotor-linked areas and greater deactivation in the DMN, ACUP sensation was associated with greater activation in higher cognitive areas: dlPFC and both the emotional/interoceptive (anterior) and cognitive/evaluative (posterior) subregions of the dmPFC. We suggest that this latter finding may be key to understanding acupuncture sensation processing in the brain, and offers clues to how the induced sensation might lead to therapeutic response.

Somatosensory sensations are a unique characteristic of acupuncture therapy. Many different styles of acupuncture attempt to elicit sensations during treatment, as they are classically thought to be linked with successful therapeutic outcomes (Cheng, 1996). When sensation was used to guide fMRI data analysis, ACUP sensation (and not SHAM) was linked with activation in both the anterior and posterior subregions of the dmPFC. Previous reviews have associated the former with emotional and interoceptive processing, and the latter with evaluative processing needed to translate a perception into a motor rating (behavioral) response (Amodio and Frith, 2006). While both ACUP and SHAM would require this evaluative processing, we believe that activity for ACUP was more pronounced due to the increased cognitive load required to rate the more complex sensations. This hypothesis is in agreement with indirect measures of cognitive load - i.e. subjects rating ACUP spent more run-time rating low and moderate sensations, and less time rating minimal/nil sensations compared to SHAM. Similarly, Kong et al. (Kong et al., 2006b) found that low and moderate pain stimuli are actually more effective than strong pain stimuli in activating the evaluative network. On the other hand, greater ACUP interoceptive processing (and likely emotional and autonomic response (Park et al., 2007)) is attributed to greater anterior dmPFC response. The dmPFC is known to connect to lower level autonomic outflow regions such as the PAG (An et al., 1998) and hypothalamus (Ongur et al., 1998) in monkeys, and has been associated with parasympathetic outflow in humans (Napadow et al., 2008). Greater emotional and interoceptive processing is likely due to the atypical stimuli coming from deeper, subdermal receptors, compared to the more commonly activated cutaneous mechanoreceptors stimulated by SHAM. We suggest that

focused bodily attention following acupuncture serves as a therapeutic mechanism for some conditions, similar to other mind-body therapies (e.g. Feldenkreis therapy, t'ai chi ch'uan) that enhance bodily awareness and have been applied for chronic pain conditions known to be linked with psychological dissociation, such as chronic pelvic pain (Haugstad et al., 2006) and fibromyalgia (Gard, 2005). In other words, acupuncture can function as a somatosensory-guided mind-body therapy.

Other potential cognitive mechanisms for acupuncture action also exist, and may have been accentuated by our percept-related fMRI approach, which effectively united a cognitive rating task with a somatosensory perception task. For instance, previous studies have found that rating pain, versus passively experiencing pain, enhances activation in most pain-matrix regions. These would include both dlPFC and dmPFC (Schoedel et al., 2008), and the enhancement is likely due to more focused attention and evaluation of the perceived pain sensation. This effect is consistent with our findings - i.e. while the sensation was different between ACUP and SHAM, it may be the reevaluation of this sensation that is even more important. In addition to dmPFC, ACUP also activated dlPFC to a greater extent than SHAM. Interestingly, this region is modulated by different forms of placebo analgesia (Kong et al., 2006a; Petrovic and Ingvar, 2002; Wager et al., 2004). One aspect of acupuncture analgesia likely involves cognitive mechanisms which may also be present in placebo interventions, and acupuncture sensation may serve to enhance this particular aspect. It should be noted that acupuncture sensation rating served to focus attention on the stimulus, leading to enhanced activation in sensorimotor as well as higher brain regions, as compared to that noted in past non-rating studies from our group (Dhond et al., 2007; Hui et al., 2005; Napadow et al., 2005). Importantly, cognition is known to strongly influence pain (for review see (Villemure and Bushnell, 2002). For instance, focused attention on pain up-regulates, while distraction down-regulates pain perception (Arntz et al., 1991). In fact, an fMRI study found that distraction leads to decreased activity in most pain-matrix regions, a phenomenon attributed to increased activation of anterior dmPFC, pgACC, and periaqueductal gray brain regions (Valet et al., 2004). Another potential mechanism for acupuncture analgesia could then involve distraction from ongoing nociceptive afference. In many styles of acupuncture, the acupuncturist commonly asks the patient whether or not needle manipulation was perceived, what the sensation felt like, etc. While such feedback is used by the acupuncturist to adjust their needle manipulation, it also draws the patient's awareness to the needle site, piquing their attention. Furthermore, many acupuncture styles use acupoint locations far away from the pain source and, at least for some localized chronic pain conditions, acupuncture analgesia may work as a distracter stimulus, interrupting or even gating chronic and pathologic "pain-matrix" activity.

Many recent clinical trials of acupuncture for chronic pain conditions have reported effectiveness of *both* real and different forms of sham acupuncture above and beyond a usual care control (Cherkin et al., 2009; Moffet, 2009; Park et al., 2008). Our fMRI results, while demonstrating interesting differences in important brain regions, also demonstrate a noted similarity between ACUP and SHAM in the brain networks modulated by the stimulus-associated sensation. In other words, whether deep or cutaneous receptors are being stimulated over an acupoint, there is sensorimotor network activation (including insula response), and DMN deactivation. Future studies should evaluate whether acupuncture sensation and activity in these networks, as induced by deep or cutaneous stimulation on or away from classical acupoints, is associated with eventual clinical outcomes. We have suggested that some bodily locations may simply be more efficient (e.g. receptor density) in maximizing afference and sensation (Napadow et al., 2009), which then induces a cascade of peripheral and brain responses potentially leading to improved clinical outcomes for some conditions. However, our study's noted similarities in brain response between ACUP and SHAM (over the same skin location) may help explain the equivalence of real and sham acupuncture in the clinical trials mentioned above, and suggests that somatosensory-based sham controls, particularly over

classical acupoints, may not be the most appropriate placebo control for future trials of acupuncture.

While some cognitive mechanisms for acupuncture action were accentuated by percept-related fMRI, our approach also introduced certain implications for the interpretation of results vis-à-vis past acupuncture fMRI studies. Specifically, compared to our current results, past studies noted not just less sensorimotor activation (as noted above), but also more prominent deactivation in subcortical and limbic brain regions for ACUP stimulation (Hui et al., 2000; Hui et al., 2005; Napadow et al., 2007; Napadow et al., 2005). The paucity of subcortical response to ACUP in our study was surprising. Several possible explanations exist. Firstly, while overlaying a cognitive task (rating) over acupuncture stimulation may have contributed to less pronounced deactivation; we did note qualitatively more prominent deactivation in our data when using the block design as GLM regressor. Hence, deactivations in subcortical regions may be due to subconscious processing during needle stimulation, which may be diminished by top-down influences from higher cortical regions responsible for evaluating needle sensation. Another possibility is that acupuncture at the acupoint used (PC-6) produces less prominent limbic deactivation - a hypothesis in agreement with the only other published fMRI report of PC-6 stimulation (Yoo et al., 2007), which noted no deactivations. On the other hand, our percept-related fMRI study demonstrated persistence of ACUP sensation into the no-stimulation rest block following needle manipulation. This persistence, if present for other acupoints as well, could have affected past block design fMRI analyses noting subcortical deactivation, as there might have been a mismatch between stimulation and afference (and sensation). This factor may also contribute to the noted inter-subject variability in fMRI response and heterogeneity of past studies (Dhond et al., 2007; Kong et al., 2007b).

We also found that SHAM sensation was associated with more prominent activation of sensorimotor brain regions (SI, SII, LOC) compared to ACUP. However, ACUP elicited stronger sensation intensity (by both average rating intensity and retrospective MASS Index) compared to SHAM. This paradox can be explained by the fact that during SHAM, subjects spent more run-time rating minimal/nil ratings. In contrast, rating ACUP sensation may be associated with greater cognitive load, as sensation intensity gradually increased throughout the run and subjects spent more run-time rating mild and moderate sensations. Thus, the SHAM sensation was easier to rate, with more discrete transitions between existent and non-existent somatosensory perception - a finding further substantiated by the significantly less power found in lower frequencies of the ratings power spectrum. This sharper transition likely resulted from more certainty in rating and allowed brain activity in sensorimotor areas to return to a “basal state” during rest blocks. This, in turn, resulted in greater dynamic range and more significant activation in the sensorimotor system for SHAM. In addition, an interesting (and previously not noted) somatosensory processing region demonstrating activation in SHAM, and not ACUP, was the LOC. This area has been associated with brain processing of both visual and tactile shape recognition (Amedi et al., 2002) - a quality typically evaluated by cutaneous receptors, which were likely more readily activated by SHAM. Other activated somatosensory areas included SI and SII. These regions have been noted in past studies to be more prominently activated for tactile stimulation compared to real acupuncture (Hui et al., 2000). We also found greater SHAM activation in the STG, a multimodal sensory area receiving input from the posterior insula (Hackett et al., 2007), which was also activated in this study. Furthermore, the pMCC, which was activated in SHAM, interacts with postero-lateral parietal regions in orienting the body in response to somatosensory stimuli (Vogt, 2005).

A similar explanation as above (for sensorimotor regions) likely also holds for greater DMN deactivation for SHAM. Specifically, greater cognitive load spread throughout the ACUP scan run and less distinct transitions between existent and non-existent sensation likely led to less pronounced deactivation of DMN brain regions such as the PCC, vmPFC, and

parahippocampus. In other words, there was significantly less time during ACUP runs when focus on an external stimulus could be switched off in preference for internal mentation, unfocused external monitoring, or any other functions attributed to the DMN (Buckner et al., 2008). However, it should also be mentioned that ACUP has been found to enhance resting connectivity in the DMN following the cessation of needle stimulation (Dhond et al., 2008), and future studies should attempt to link this lasting influence on the DMN with brain response to active stimulation.

Several limitations to our approach should be discussed. Firstly, in addition to the overlay of a cognitive task on top of a somatosensory task, percept-related fMRI is also associated with a motor task - i.e. the right-handed rating of sensation using our MR-compatible potentiometer device. Hence, some of our fMRI results may have been influenced by brain networks needed to execute this motor task. Particularly, activation in contralateral M1 and SI (left precentral and postcentral gyri) and deactivation in ipsilateral SI (right BA 3a) for both ACUP and SHAM (though greater in SHAM) was likely due to the execution of the motor aspect of sensation rating. Similarly, brain response in the cuneus and other visual areas of the medial occipital lobe are likely due to the visual feedback inherent to the rating task. These limitations have been noted in the past, and our analysis used a control condition (SHAM) to attempt to subtract off or minimize the motor/rating and visual aspects of the task. Furthermore, we (and others, see (Baliki et al., 2006; Davis et al., 2002) believe that these disadvantages are outweighed by the advantages of collecting, analyzing, and using on-line ratings to guide fMRI data analysis, which uniquely allows for the direct inference of the neural correlates of sensation.

In conclusion, percept-related fMRI demonstrated that sensations elicited in real ACUP are qualitatively more complex, more persistent, and vary more appreciably between individuals, compared to SHAM. Furthermore, while both ACUP and SHAM elicited sensation associated with activation of the sensorimotor system and deactivation of the DMN, important differences were also found. SHAM sensation was associated with greater activation in the sensorimotor system and greater deactivation in the DMN compared to ACUP, a consequence of more distinct transitions between existent and non-existent sensation. However, an increased cognitive load for subjects rating ACUP sensations led to greater activation in the dlPFC, and both the emotional/interoceptive (anterior) and cognitive/evaluative (posterior) subregions of the dmPFC. This latter finding may be a salient component of acupuncture analgesia - sensations focus attention and accentuate bodily awareness, contributing to enhanced top-down modulation of nociceptive afference and central pain networks.

Supplementary Material

Refer to Web version on PubMed Central for supplementary material.

ACKNOWLEDGEMENTS

We would like to thank the National Center for Complementary & Alternative Medicine, NIH for funding support: K01-AT002166, R01-AT004714 (Napadow), P01-AT002048 (Rosen), K01-AT004481 (Dhond), K01-AT01111 (Harris) and F05-AT003770 (Park). We also acknowledge the NCRN (P41-RR14075, GCRC M01-RR01066), the Mental Illness and Neuroscience Discovery (MIND) Institute. Dr. Park was also supported by the Institute of Information Technology Advancement, Korea IITA-2008-(C1090-0801-0002). Dr. Harris was also supported by Department of Army grant DAMD-Award Number W81XWH-07-2-0050, and Dana Foundation Award in Brain and Immuno-imaging. We would also like to thank Bruce Rosen and Ted Kaptchuk (K24-AT004095) for helpful comments on the interpretation of our data. The content is solely the responsibility of the authors and does not necessarily represent the official views of our funding agencies.

REFERENCES

- Amedi A, Jacobson G, Hendler T, Malach R, Zohary E. Convergence of visual and tactile shape processing in the human lateral occipital complex. *Cereb Cortex* 2002;12:1202–1212. [PubMed: 12379608]
- Amodio DM, Frith CD. Meeting of minds: the medial frontal cortex and social cognition. *Nat Rev Neurosci* 2006;7:268–277. [PubMed: 16552413]
- An X, Bandler R, Ongur D, Price JL. Prefrontal cortical projections to longitudinal columns in the midbrain periaqueductal gray in macaque monkeys. *J Comp Neurol* 1998;401:455–479. [PubMed: 9826273]
- Arntz A, Dreesen L, Merckelbach H. Attention, not anxiety, influences pain. *Behav Res Ther* 1991;29:41–50. [PubMed: 2012588]
- Baliki MN, Chialvo DR, Geha PY, Levy RM, Harden RN, Parrish TB, Apkarian AV. Chronic pain and the emotional brain: specific brain activity associated with spontaneous fluctuations of intensity of chronic back pain. *J Neurosci* 2006;26:12165–12173. [PubMed: 17122041]
- Buckner RL, Andrews-Hanna JR, Schacter DL. The brain's default network: anatomy, function, and relevance to disease. *Ann N Y Acad Sci* 2008;1124:1–38. [PubMed: 18400922]
- Cheng, X. Chinese Acupuncture and Moxibustion. Beijing Foreign Languages Press; Beijing: 1996.
- Cherkin DC, Sherman KJ, Avins AL, Erro JH, Ichikawa L, Barlow WE, Delaney K, Hawkes R, Hamilton L, Pressman A, Khalsa PS, Deyo RA. A randomized trial comparing acupuncture, simulated acupuncture, and usual care for chronic low back pain. *Arch Intern Med* 2009;169:858–866. [PubMed: 19433697]
- Dale AM, Fischl B, Sereno MI. Cortical surface-based analysis. I. Segmentation and surface reconstruction. *Neuroimage* 1999;9:179–194. [PubMed: 9931268]
- Davis KD, Pope GE, Crawley AP, Mikulis DJ. Neural correlates of prickle sensation: a percept-related fMRI study. *Nat Neurosci* 2002;5:1121–1122. [PubMed: 12368810]
- Dhond RP, Kettner N, Napadow V. Neuroimaging acupuncture effects in the human brain. *J Altern Complement Med* 2007;13:603–616. [PubMed: 17718643]
- Dhond RP, Yeh C, Park K, Kettner N, Napadow V. Acupuncture modulates resting state connectivity in default and sensorimotor brain networks. *Pain* 2008;136:407–418. [PubMed: 18337009]
- Fischl B, Sereno MI, Tootell RB, Dale AM. High-resolution intersubject averaging and a coordinate system for the cortical surface. *Hum Brain Mapp* 1999;8:272–284. [PubMed: 10619420]
- Gard G. Body awareness therapy for patients with fibromyalgia and chronic pain. *Disabil Rehabil* 2005;27:725–728. [PubMed: 16012065]
- Hackett TA, Smiley JF, Ulbert I, Karmos G, Lakatos P, de la Mothe LA, Schroeder CE. Sources of somatosensory input to the caudal belt areas of auditory cortex. *Perception* 2007;36:1419–1430. [PubMed: 18265825]
- Haugstad GK, Haugstad TS, Kirste UM, Leganger S, Wojniusz S, Klemmetsen I, Malt UF. Posture, movement patterns, and body awareness in women with chronic pelvic pain. *J Psychosom Res* 2006;61:637–644. [PubMed: 17084141]
- Ho TJ, Duann JR, Chen CM, Chen JH, Shen WC, Lu TW, Liao JR, Lin JG. Carryover effects alter fMRI statistical analysis in an acupuncture study. *Am J Chin Med* 2008;36:55–70. [PubMed: 18306450]
- Hui KK, Liu J, Makris N, Gollub RL, Chen AJ, Moore CI, Kennedy DN, Rosen BR, Kwong KK. Acupuncture modulates the limbic system and subcortical gray structures of the human brain: evidence from fMRI studies in normal subjects. *Hum Brain Mapp* 2000;9:13–25. [PubMed: 10643726]
- Hui KK, Liu J, Marina O, Napadow V, Haselgrove C, Kwong KK, Kennedy DN, Makris N. The integrated response of the human cerebro-cerebellar and limbic systems to acupuncture stimulation at ST 36 as evidenced by fMRI. *Neuroimage* 2005;27:479–496. [PubMed: 16046146]
- Hui KK, Nixon EE, Vangel MG, Liu J, Marina O, Napadow V, Hodge SM, Rosen BR, Makris N, Kennedy DN. Characterization of the “Deqi” Response in Acupuncture. *BMC Complement Altern Med* 2007;7:33. [PubMed: 17973984]

- Kong J, Fufa DT, Gerber AJ, Rosman IS, Vangel MG, Gracely RH, Gollub RL. Psychophysical outcomes from a randomized pilot study of manual, electro, and sham acupuncture treatment on experimentally induced thermal pain. *J Pain* 2005;6:55–64. [PubMed: 15629419]
- Kong J, Gollub R, Huang T, Polich G, Napadow V, Hui K, Vangel M, Rosen B, Kaptchuk TJ. Acupuncture de qi, from qualitative history to quantitative measurement. *J Altern Complement Med* 2007a; 13:1059–1070. [PubMed: 18166116]
- Kong J, Gollub RL, Rosman IS, Webb JM, Vangel MG, Kirsch I, Kaptchuk TJ. Brain activity associated with expectancy-enhanced placebo analgesia as measured by functional magnetic resonance imaging. *J Neurosci* 2006a;26:381–388. [PubMed: 16407533]
- Kong J, Gollub RL, Webb JM, Kong JT, Vangel MG, Kwong K. Test-retest study of fMRI signal change evoked by electroacupuncture stimulation. *Neuroimage* 2007b;34:1171–1181. [PubMed: 17157035]
- Kong J, White NS, Kwong KK, Vangel MG, Rosman IS, Gracely RH, Gollub RL. Using fMRI to dissociate sensory encoding from cognitive evaluation of heat pain intensity. *Hum Brain Mapp* 2006b;27:715–721. [PubMed: 16342273]
- Langevin HM, Churchill DL, Wu J, Badger GJ, Yandow JA, Fox JR, Krag MH. Evidence of connective tissue involvement in acupuncture. *Faseb J* 2002;16:872–874. [PubMed: 11967233]
- Moffet HH. Sham acupuncture may be as efficacious as true acupuncture: a systematic review of clinical trials. *J Altern Complement Med* 2009;15:213–216. [PubMed: 19250001]
- Napadow V, Dhond R, Conti G, Makris N, Brown EN, Barbieri R. Brain correlates of autonomic modulation: combining heart rate variability with fMRI. *Neuroimage* 2008;42:169–177. [PubMed: 18524629]
- Napadow V, Dhond R, Park K, Kim J, Makris N, Kwong KK, Harris RE, Purdon PL, Kettner N, Hui KK. Time-variant fMRI activity in the brainstem and higher structures in response to acupuncture. *Neuroimage*. 2009
- Napadow V, Kettner N, Liu J, Li M, Kwong KK, Vangel M, Makris N, Audette J, Hui KK. Hypothalamus and amygdala response to acupuncture stimuli in Carpal Tunnel Syndrome. *Pain* 2007;130:254–266. [PubMed: 17240066]
- Napadow V, Makris N, Liu J, Kettner NW, Kwong KK, Hui KK. Effects of electroacupuncture versus manual acupuncture on the human brain as measured by fMRI. *Hum Brain Mapp* 2005;24:193–205. [PubMed: 15499576]
- Ojemann JG, Akbudak E, Snyder AZ, McKinstry RC, Raichle ME, Conturo TE. Anatomic localization and quantitative analysis of gradient refocused echo-planar fMRI susceptibility artifacts. *Neuroimage* 1997;6:156–167. [PubMed: 9344820]
- Oldfield RC. The assessment and analysis of handedness: the Edinburgh inventory. *Neuropsychologia* 1971;9:97–113. [PubMed: 5146491]
- Ongur D, An X, Price JL. Prefrontal cortical projections to the hypothalamus in macaque monkeys. *J Comp Neurol* 1998;401:480–505. [PubMed: 9826274]
- Park H, Park J, Lee H. Does Deqi (needle sensation) exist? *Am J Chin Med* 2002;30:45–50. [PubMed: 12067096]
- Park J, Linde K, Manheimer E, Molsberger A, Sherman K, Smith C, Sung J, Vickers A, Schnyer R. The status and future of acupuncture clinical research. *J Altern Complement Med* 2008;14:871–881. [PubMed: 18803496]
- Park, K.; Kim, J.; Napadow, V. Year. Verum Versus Placebo: Orienting Responses for Acupuncture Induced Autonomic Outflow to the Heart and Eye in Humans. Society for Acupuncture Research Annual Conference; Journal of Alternative and Complementary Medicine: Baltimore, MD; p. 853-862.
- Petrovic P, Ingvar M. Imaging cognitive modulation of pain processing. *Pain* 2002;95:1–5. [PubMed: 11790461]
- Raichle ME, MacLeod AM, Snyder AZ, Powers WJ, Gusnard DA, Shulman GL. A default mode of brain function. *Proc Natl Acad Sci U S A* 2001;98:676–682. [PubMed: 11209064]
- Sandberg M, Lundeberg T, Lindberg LG, Gerdle B. Effects of acupuncture on skin and muscle blood flow in healthy subjects. *Eur J Appl Physiol* 2003;90:114–119. [PubMed: 12827364]

- Schoedel AL, Zimmermann K, Handwerker HO, Forster C. The influence of simultaneous ratings on cortical BOLD effects during painful and non-painful stimulation. *Pain* 2008;135:131–141. [PubMed: 17611034]
- Steele JD, Lawrie SM. Segregation of cognitive and emotional function in the prefrontal cortex: a stereotactic meta-analysis. *Neuroimage* 2004;21:868–875. [PubMed: 15006653]
- Valet M, Sprenger T, Boecker H, Willloch F, Rummeny E, Conrad B, Erhard P, Tolle TR. Distraction modulates connectivity of the cingulo-frontal cortex and the midbrain during pain--an fMRI analysis. *Pain* 2004;109:399–408. [PubMed: 15157701]
- Villemure C, Bushnell MC. Cognitive modulation of pain: how do attention and emotion influence pain processing? *Pain* 2002;95:195–199. [PubMed: 11839418]
- Vincent CA, Richardson PH, Black JJ, Pither CE. The significance of needle placement site in acupuncture. *J Psychosom Res* 1989;33:489–496. [PubMed: 2795521]
- Vogt BA. Pain and emotion interactions in subregions of the cingulate gyrus. *Nat Rev Neurosci* 2005;6:533–544. [PubMed: 15995724]
- Wager TD, Rilling JK, Smith EE, Sokolik A, Casey KL, Davidson RJ, Kosslyn SM, Rose RM, Cohen JD. Placebo-induced changes in FMRI in the anticipation and experience of pain. *Science* 2004;303:1162–1167. [PubMed: 14976306]
- Wang KM, Yao SM, Xian YL, Hou ZL. A study on the receptive field of acupoints and the relationship between characteristics of needling sensation and groups of afferent fibres. *Sci Sin [B]* 1985;28:963–971.
- Wang SM, Constable RT, Tokoglu FS, Weiss DA, Freyle D, Kain ZN. Acupuncture-induced blood oxygenation level-dependent signals in awake and anesthetized volunteers: a pilot study. *Anesth Analg* 2007;105:499–506. [PubMed: 17646512]
- Yoo SS, Kerr CE, Park M, Im DM, Blinder RA, Park H, Kaptchuk TJ. Neural activities in human somatosensory cortical areas evoked by acupuncture stimulation. *Complement Ther Med* 2007;15:247–254. [PubMed: 18054726]

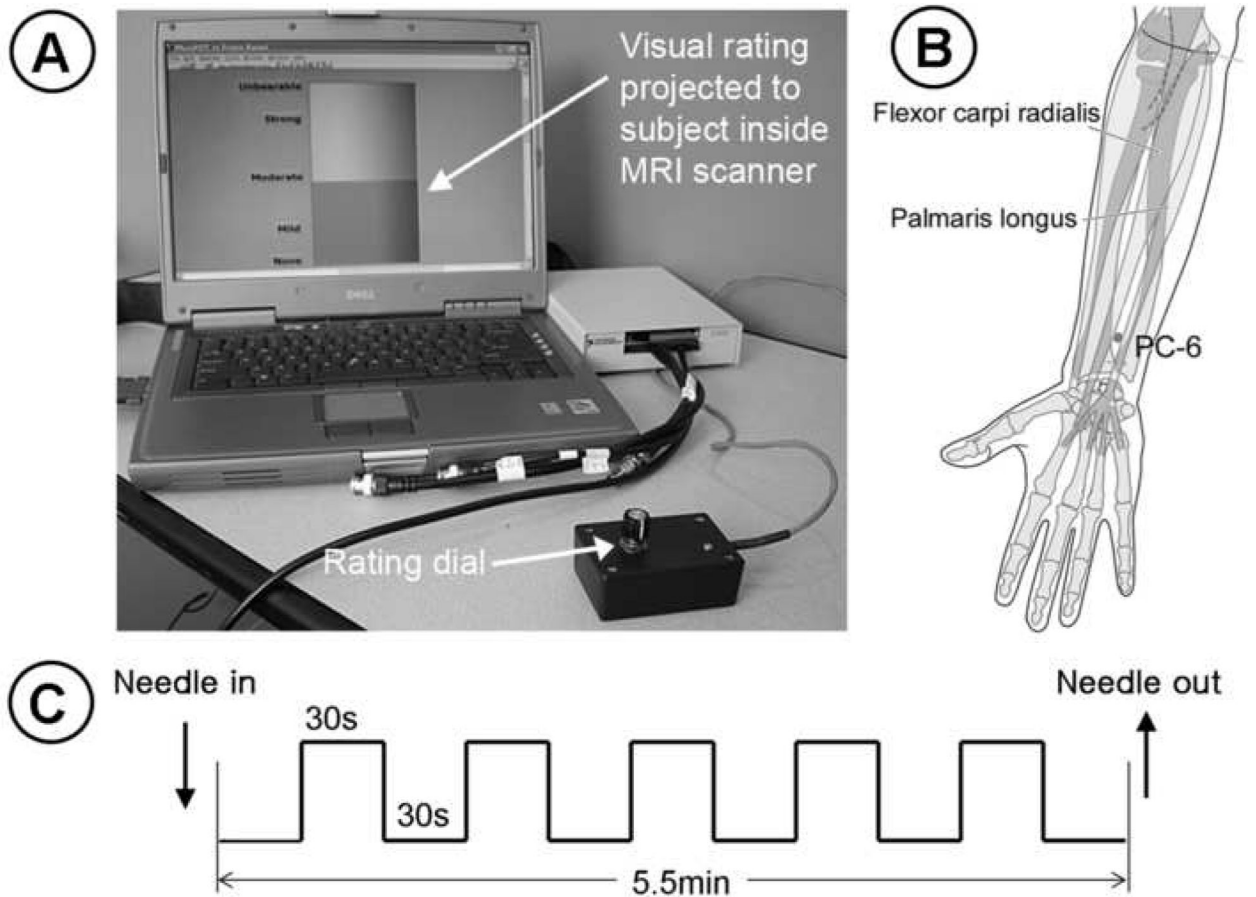


Figure 1. Experimental protocol. (A) A MR-compatible handheld potentiometer and rating dial was employed for online rating of acupuncture sensation. (B) Stimulation location (PC-6) for both real (ACUP) and sham (SHAM) acupuncture. (C) The fMRI block design paradigm consisted of alternating 30sec stimulation with 30sec rest blocks for both ACUP and SHAM. n.b. figure in (B) was modified from a image in `WHO Regional Office for the Western Pacific, 2008, WHO Standard Acupuncture Point Locations in the Western Pacific Region, Manila'

Online Psychophysics

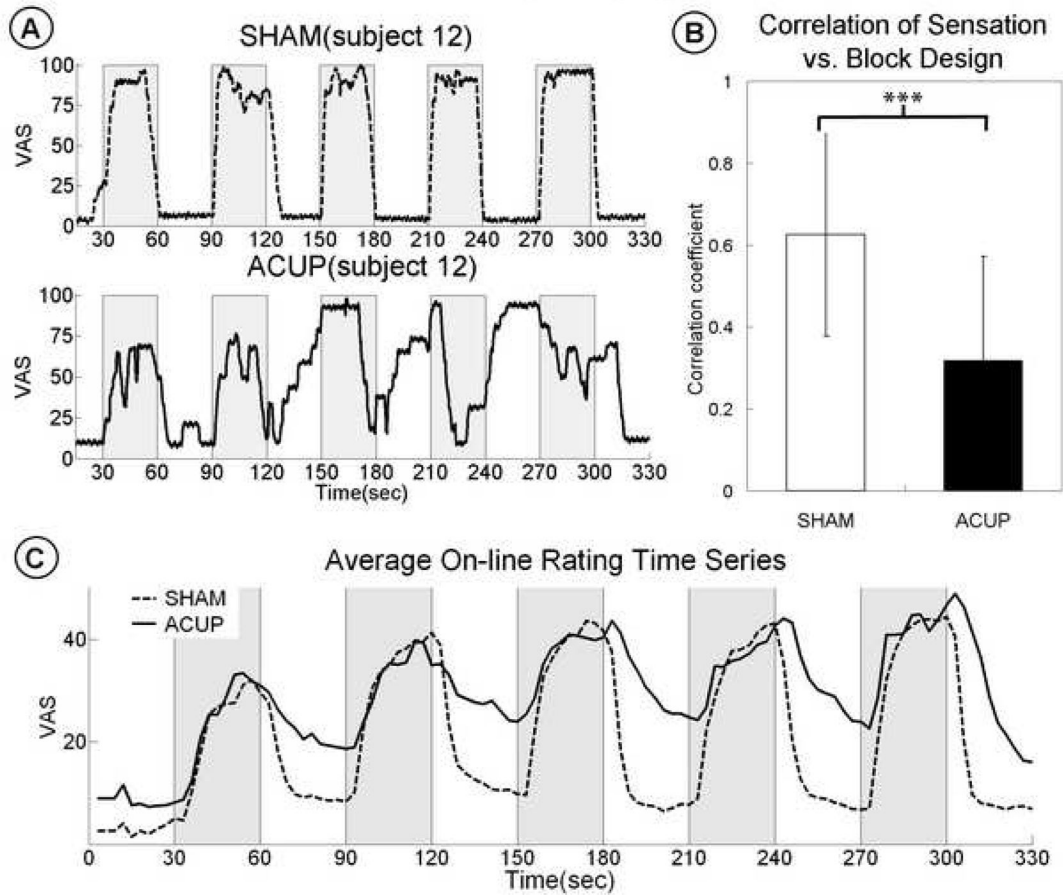


Figure 2.

(A) In a single subject, SHAM induced on-line sensation that followed the stimulation paradigm more closely than for ACUP, where sensation was even noted to peak during a rest block. (B) Group analysis demonstrated greater correlation between on-line sensation and the stimulation paradigm for SHAM, compared to ACUP. (C) Group-averaged timeseries for ACUP and SHAM. Compared to SHAM, ACUP demonstrated both greater persistence of sensation into nonstimulation rest blocks and a gradual increase of sensation across the scan run. n.b. error bars in (B) represent standard deviation. *** $p < 0.001$

Online Psychophysics: Spectral Analysis

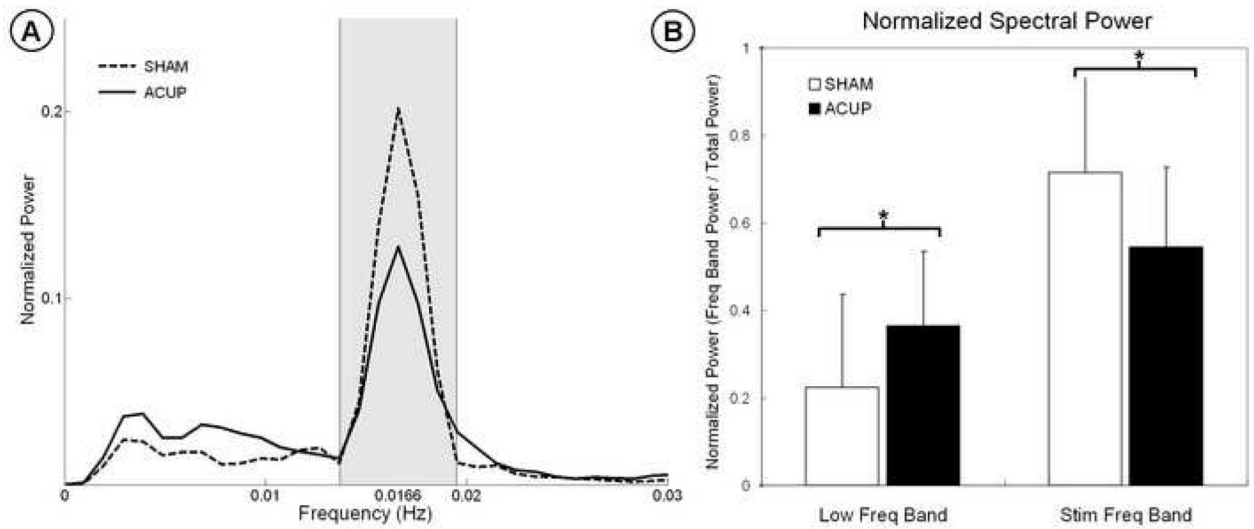


Figure 3. Spectral analysis of online sensation ratings. (A) Average spectra for both ACUP and SHAM demonstrated a large peak in the stimulation frequency band (0.01366-0.01966Hz?). (B) SHAM demonstrated greater power in the stimulation frequency band, while ACUP demonstrated greater power in a lower frequency band, below the stimulation band. n.b error bars in (B) represent standard deviation. * $p < 0.05$

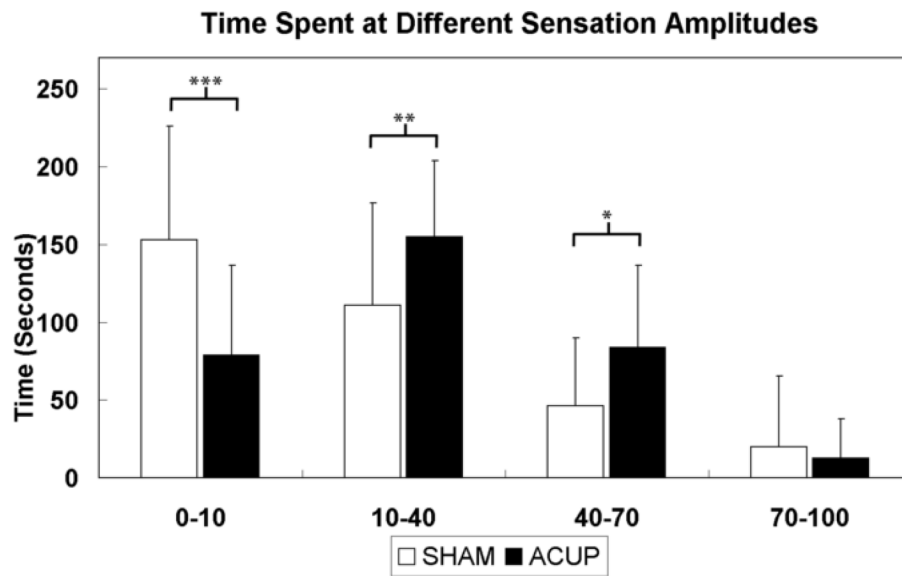


Figure 4.

Cognitive load was inferred from the amount of time subjects spent rating different sensation intensities. For ACUP, subjects spent more of the scan run (330sec total) rating both low (10-40) and moderate (40-70) sensations than for SHAM. In turn, subjects experiencing SHAM spent more time rating minimal to no sensation (0-10). No difference was found for strong sensations. n.b. error bars represent standard deviation. *** $p < 0.001$, ** $p < 0.005$, * $p < 0.05$

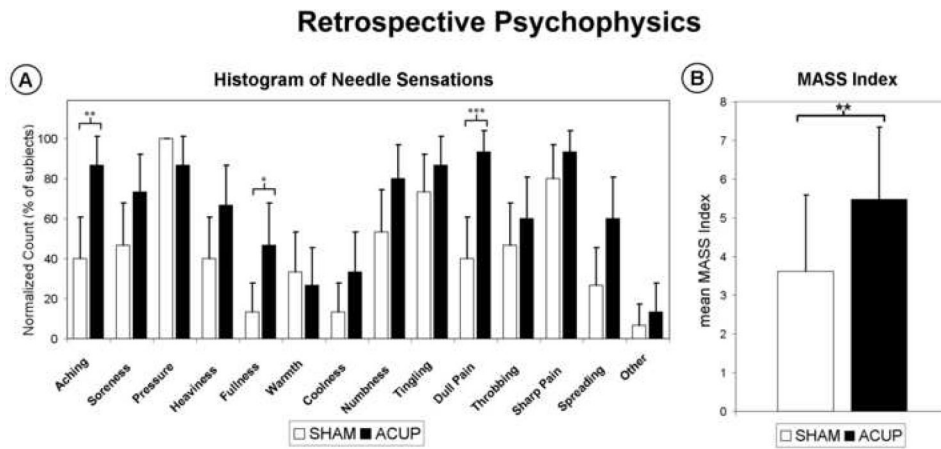


Figure 5. Retrospective psychophysical analysis using the MASS scale. (A) Differences in the types of sensations elicited (expressed as a histogram) were found between ACUP and Sham. ACUP more frequently induced “aching”, “fullness”, and “dull pain”. (B) MASS index, a summary measure of sensation intensity, was greater for ACUP compared to SHAM. n.b. Error bars in (A) represent a 90% confidence interval for binomial distribution. Sensations on the abscissa are in the order presented to the subjects. Error bars in (B) represent standard deviation. * $p < 0.05$, ** $p < 0.01$, *** $p < 0.005$.

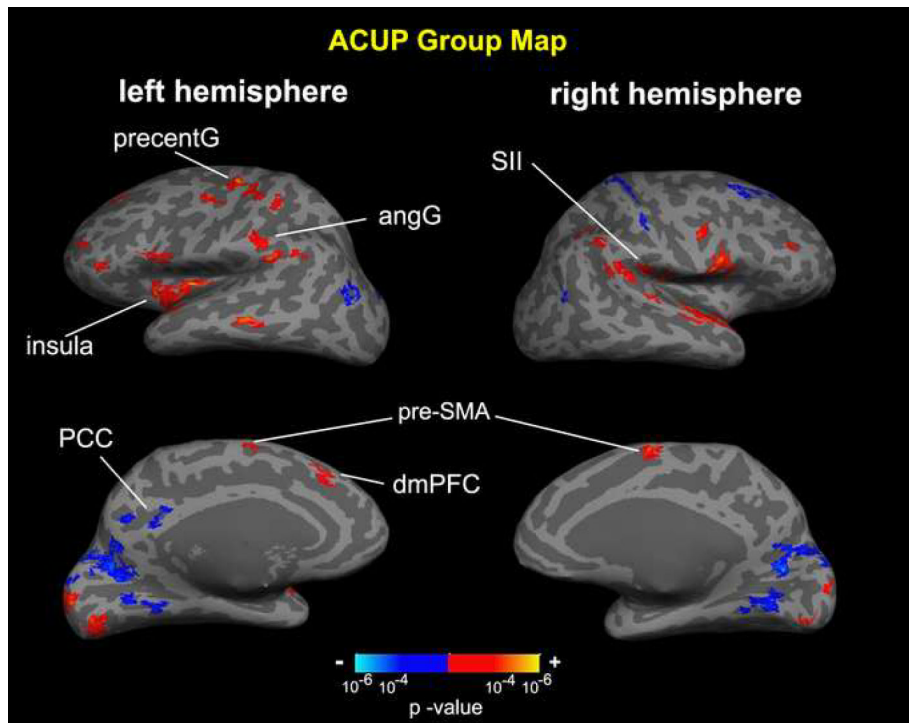


Figure 6. Percept-related fMRI main effect group map for ACUP. Percept-related fMRI using on-line sensation rating yielded activation in sensorimotor processing regions (SII, angG, insula, precentG) and deactivation in default mode regions (e.g. PCC). Higher cognitive areas (e.g. dmPFC, dlPFC) were also modulated. PCC = posterior cingulate cortex, SMA = supplementary motor area, dmPFC = dorsomedial prefrontal cortex, precentG = precentral gyrus, angG = angular gyrus, SII = secondary somatosensory cortex.

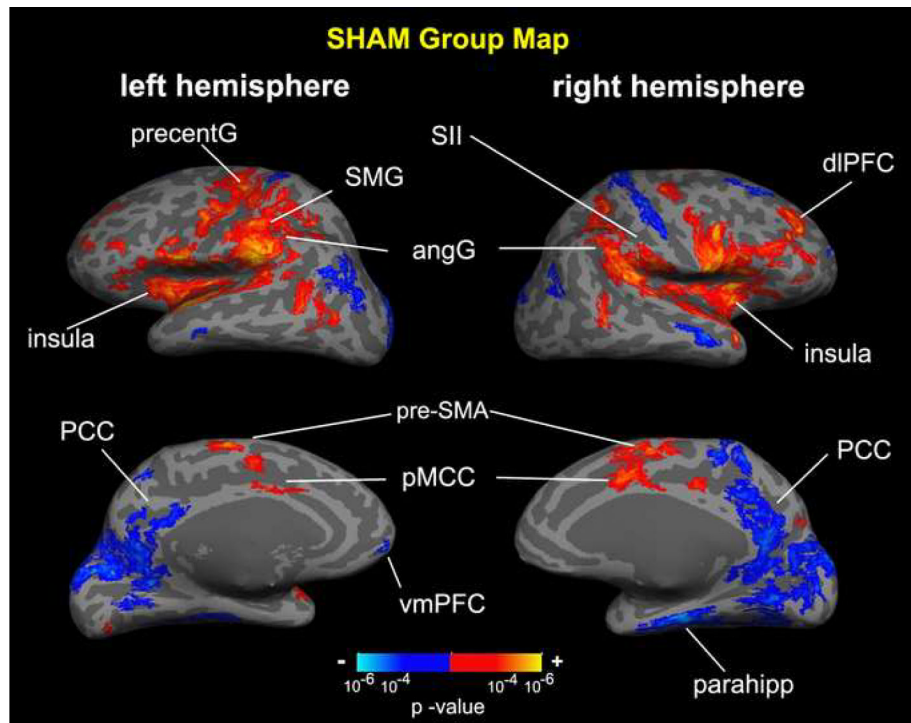


Figure 7. Percept-related fMRI main effect group map for SHAM. Percept-related fMRI using on-line sensation rating yielded activation in sensorimotor processing regions (SII, angG, insula, SMG, precentG, pMCC) and deactivation in default mode regions (e.g. PCC, vmPFC, parahipp). Higher cognitive areas (e.g. dIPFC) were also modulated. PCC = posterior cingulate cortex; pMCC = posterior middle cingulate cortex; SMA = supplementary motor area; dIPFC, vmPFC = dorsolateral, ventromedial prefrontal cortex; precentG = precentral gyrus; angG = angular gyrus; SII = secondary somatosensory cortex; SMG = supramarginal gyrus.

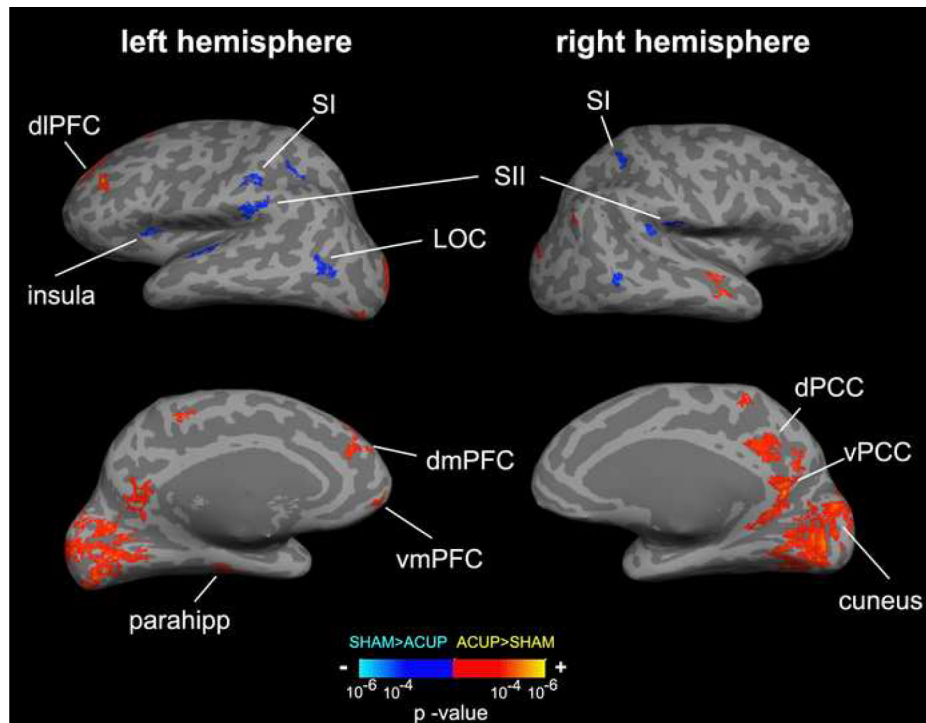


Figure 8. Percept-related fMRI group difference map for ACUP-SHAM. Using on-line sensation rating, SHAM induced greater activation in sensorimotor processing regions (SI, SII, insula, LOC) and greater deactivation in default mode regions (e.g. PCC, vmPFC, parahipp). However, ACUP induced greater activation in cognitive-evaluative (posterior dmPFC, dIPFC) and emotionalinteroceptive (anterior dmPFC) cortical brain regions. n.b. PCC = posterior cingulate cortex; dIPFC, dmPFC, vmPFC = dorsolateral, dorsomedial, ventromedial prefrontal cortex; LOC = lateral occipital complex; SI, SII = primary, secondary somatosensory cortex.

Table 1
Summary of percept-fMRI main effect map for ACUP

	Side	Location (Talairach)			Z-score	Size (mm ² or mm ³)	% change (mean±sd)
		X(mm)	Y(mm)	Z(mm)			
SI	R	20	-28	64	< -3.89	218.6	-0.51±0.18
	L	-42	-31	53	3.54	118.8	0.91±0.21
SII	R	49	-20	18	> 3.89	119.1	0.76±0.34
	L	-54	-35	32	3.62	130.9	0.92±0.25
angular gyrus	R	54	-43	37	> 3.89	120.7	1.02±0.14
	L	-60	-29	32	> 3.89	134.0	1.14±0.22
superior parietal	R	38	-46	40	2.32	66.6	1.32±0.17
	R	52	-8	-1	> 3.89	399.8	1.42±0.71
STG	R	53	5	8	> 3.89	514.2	1.10±0.33
	L	-51	13	2	> 3.89	282.6	0.98±0.24
frontal operculum	R	42	-3	-16	3.43	94.3	0.84±0.24
	L	-37	-8	3	> 3.89	625.7	0.92±0.28
ant+post insula	L	-30	-12	58	> 3.89	133.3	0.91±0.31
	R	8	12	53	> 3.89	169.1	1.18±0.23
precentral gyrus	L	-6	13	56	2.08	68.5	1.02±0.23
	L	-7	-35	38	-3.43	107.9	-0.40±0.14
dPCC (BA23)	L	-10	-53	39	-3.39	105.1	-0.55±0.18
	R	41	-64	25	-2.98	83.9	-0.47±0.13
IPL	L	-36	-84	28	< -3.89	196.4	-0.43±0.18
	R	10	-59	9	< -3.89	342.8	-0.53±0.20
lingual gyrus	L	-16	-54	-4	< -3.89	139.5	-0.49±0.13
	R	29	31	38	< -3.89	201.9	-0.78±0.20
dIPFC	R	38	42	8	> 3.89	113.5	1.10±0.21
	L	-45	36	-9	2.78	89.1	1.16±0.34
dmPFC	L	-10	39	23	2.98	95.3	0.57±0.20
	L	-64	-38	-6	2.35	76.0	0.83±0.21
MTG	R	10	-96	21	2.89	81.0	1.69±0.59
	L	-4	-92	8	> 3.89	359.0	1.17±0.35

IPL: inferior parietal lobule, MTG: middle temporal gyrus, dPCC: dorsal posterior cingulate cortex, dlPFC: dorsolateral prefrontal cortex, dmPFC: dorsomedial prefrontal cortex, SI: primary somatosensory cortex, SII: secondary somatosensory cortex, SMA: supplementary motor area, STG: superior temporal gyrus.

Table 2
Summary of percept-related fMRI main effect map for SHAM

	Side	Location (Talairach)			Z (mm)	Z-score	Size (mm ² or mm ³)	% change (mean±sd)
		X (mm)	y (mm)	Z (mm)				
SI	R	39	-23	47	< -3.89	276.0	-1.68±0.55	
	R	30	-39	50	> 3.89	106.4	2.18±0.81	
SII	R	51	-34	21	> 3.89	1621.3	2.18±0.81	
	L	-53	-27	20	> 3.89	4215.7	1.83±0.87	
STG	L	-57	-44	15	2.33	75.7	1.01±0.47	
	R	62	-51	5	> 3.89	79.9	1.42±0.36	
LOC	L	-44	-68	11	3.62	111.2	0.91±0.34	
	R	60	6	12	> 3.89	1444.3	1.67±0.61	
frontal operculum	L	-52	4	6	> 3.89	944.5	1.35±0.58	
	R	35	16	0	> 3.89	384.5	1.54±0.53	
anterior insula	R	39	-8	0	> 3.89	169.4	1.20±0.24	
posterior insula	L	-39	-14	6	> 3.89	2117.0	1.60±0.76	
ant+post insula	L	-5	13	30	2.39	77.4	1.15±0.46	
aMCC	R	6	17	29	> 3.89	169.5	1.46±0.38	
pMCC	R	35	-8	50	> 3.89	70.7	1.20±0.54	
precentral gyrus	L	-37	-9	57	> 3.89	2080.8	1.54±0.69	
	R	9	9	49	> 3.89	113.9	1.07±0.35	
pre-SMA	L	-10	0	59	> 3.89	202.1	2.01±0.52	
	R	7	-39	39	< -3.89	128.5	-1.57±0.45	
dPCC	L	-4	-46	27	< -3.89	304.7	-1.61±0.62	
	R	14	-45	31	< -3.89	48.3	-1.88±0.22	
vPCC	R	6	-55	26	< -3.89	516.2	-1.46±0.43	
precuneus	L	-11	-44	63	-2.99	93.6	-1.10±0.54	
	L	-7	52	-16	-3.72	120.2	-2.30±0.81	
vmPFC	R	39	-75	35	-2.96	49.8	-1.75±0.25	
IPL	L	-39	-53	22	< -3.89	1126.8	-1.57±0.83	
MTG	R	56	-7	-20	< -3.89	140.9	-0.78±0.28	
hippocampal formation	R	34	-28	-10	-2.99	4136.0	-0.42±0.11	

	Side	Location (Talairach)			Z (mm)	Z-score	Size (mm ² or mm ³)	%change (mean±sd)
		X (mm)	y (mm)	Z (mm)				
parahippocampus	R	32	-31	-13	< -3.89	452.8	-0.75±0.30	
lingual gyrus	R	8	-59	7	< -3.89	174.1	-1.48±0.37	
dlPFC	R	35	44	20	> 3.89	308.8	1.49±0.42	
	L	-44	34	5	> 3.89	145.1	1.18±0.62	
cuneus	R	10	-85	25	< -3.89	1334.3	-1.62±0.72	
	L	-4	-75	25	< -3.89	3477.6	-1.32±0.77	
caudate nucleus	R	16	18	8	2.85	920.0	0.51±0.11	
	L	-10	8	10	2.8	352.0	0.49±0.10	
putamen	R	26	-2	2	2.84	2096.0	0.48±0.11	
	L	-24	6	8	2.98	2568.0	0.49±0.15	
cerebellum	L	-30	-60	-24	2.94	6728.0	0.58±0.19	

LOC: lateral occipital complex, aMCC: anterior midcingulate cortex, pMCC: post prefrontal cortex, IPL: inferior parietal lobule, MTG: middle temporal gyrus, dPCC: dorsal posterior cingulate cortex, vPCC: ventral posterior cingulate cortex, dlPFC: dorsolateral prefrontal cortex, vmPFC: ventromedial prefrontal cortex, SI: primary somatosensory cortex, SII: secondary somatosensory cortex, SMA: supplementary motor area, STG: superior temporal gyrus.

Table 3

Summary of percept-fMRI difference map (ACUP-SHAM)

	Side	Location (Talairach)			Z (mm)	Z-score	Size (mm ²)	ACUP (mean±sd)	SHAM (mean±sd)
		X (mm)	Y (mm)	Z (mm)					
SI(BA2)	R	31	-39	50	-2.28	70.6	0.16±0.23	2.87±0.99	
	L	-54	-23	41	-3.48	109.2	0.60±0.33	3.01±0.66	
SII	R	48	-34	20	-3.23	98.6	1.05±0.56	4.11±0.67	
	L	-51	-28	20	< -3.89	241.4	0.80±0.44	4.45±0.89	
medial parietal	R	5	-31	53	2.10	66.0	0.35±0.39	-1.51±0.61	
	L	-7	-26	51	2.12	66.0	0.27±0.34	-1.16±0.54	
MTG/STG	R	56	-7	-20	2.12	66.4	-0.24±0.24	-2.49±1.00	
	L	-55	-7	0	> 3.89	127.2	0.35±0.47	-3.29±1.06	
LOC	R	57	-59	3	-2.70	82.4	-0.15±0.30	1.86±1.03	
	L	-44	-69	10	-3.05	91.0	0.02±0.20	1.81±0.66	
anterior insula	L	-30	14	5	-3.32	102.0	-0.46±0.54	1.87±1.02	
	R	10	-54	19	> 3.89	434.2	-0.69±0.48	-2.46±0.74	
vPCC (BA23)	L	-6	-49	20	> 3.89	282.7	-0.46±0.45	-2.32±0.82	
dPCC (BA23)	R	9	-41	31	> 3.89	344.0	-0.22±0.39	-1.90±0.75	
	R	6	-56	36	3.32	106.1	-0.47±0.59	-1.47±0.87	
precuneus	R	6	-56	36	3.32	106.1	-0.47±0.59	-1.47±0.87	
vmPFC	L	-6	54	-17	2.98	89.3	1.20±0.39	-1.69±1.16	
	R	45	-65	31	2.12	66.5	-0.17±0.17	-1.16±0.29	
IPL	L	-31	-31	-13	2.07	64.9	-0.07±0.26	-2.41±0.54	
	L	-22	49	15	3.62	112.5	1.10±0.43	-0.43±0.57	
parahippocampus	L	-31	-31	-13	2.07	64.9	-0.07±0.26	-2.41±0.54	
dlPFC	L	-22	49	15	3.62	112.5	1.10±0.43	-0.43±0.57	
	L	-13	46	9	2.12	65.9	0.88±0.53	0.23±0.25	
dmPFC	R	19	-72	-2	> 3.89	2997.5	-0.30±0.89	-1.89±0.86	
	L	-11	-95	-5	> 3.89	1624.2	0.44±0.92	-0.72±0.84	

IPL: inferior parietal lobule, LOC: lateral occipital complex, MTG: middle temporal gyrus, dPCC: dorsal posterior cingulate cortex, vPCC: ventral posterior cingulate cortex, dlPFC: dorsolateral prefrontal cortex, dmPFC: dorsomedial prefrontal cortex, vmPFC: ventromedial prefrontal cortex, SI: primary somatosensory cortex, SII: secondary somatosensory cortex, STG: superior temporal gyrus.